Dalton Transactions

ROYAL SOCIETY OF CHEMISTRY

PAPER

View Article Online
View Journal | View Issue

Check for updates

Cite this: *Dalton Trans.*, 2025, **54**, 6261

Alkylamido lutetium complexes as prospective lutetium imido precursors: synthesis, characterization and ligand design†

Jackson P. Knott, Shou-Jen Hsiang and Paul G. Hayes *

Received 12th February 2025,
Accepted 19th March 2025

DOI: 10.1039/d5dt00338e

rsc.li/dalton

Mixed alkylamido lutetium complexes, $L^{iPr}Lu(CH_2SiMe_3)(NHCPh_3)$ (**7$_{CPh3}$**) and $L^{iPr}Lu(CH_2SiMe_3)(NHDipp)$ (**7$_{Dipp}$**) (L^{iPr} = 2,5-[$^{i}Pr_2P$ = N(4-$^{i}PrC_6H_4$)]$_2C_4H_2N^-$), were synthesized by addition of a bulky primary amine, NH_2R (R = CPh_3, Dipp) (Dipp = 2,6-$^{i}Pr_2C_6H_3$) to the dialkyl complex $L^{iPr}Lu(CH_2SiMe_3)_2$ (**6**). Unlike complexes supported by the related pincer ligand L^{Ph} (L^{Ph} = 2,5-[Ph_2P = N(4-$^{i}PrC_6H_4$)]$_2C_4H_2N^-$) these species proved resistant to C–H cyclometalative processes. Attempts to access lutetium imdes *via* addition of 4-dimethylaminopyridine (DMAP) to **7$_{CPh3}$** and **7$_{Dipp}$** promoted disproportionation, affording 0.5 equivalents of the corresponding bisamide complexes $L^{iPr}Lu(NHCPh_3)_2$ (**8$_{CPh3}$**) and $L^{iPr}Lu(NHDipp)_2$ (**8$_{Dipp}$**), respectively, as well as 0.5 equivalents of $L^{iPr}Lu(CH_2SiMe_3)_2$, which decomposed in the presence of DMAP. Incorporation of internal Lewis bases was accomplished by replacing the *N*-aryl substituents in L^{iPr} with 4,6-dimethylpyrimidine groups (L^{Pm}, **11**). The correspondng dialkyl lutetium complex $L^{Pm}Lu(CH_2SiMe_3)_2$ (**12**) was prepared, from which loss of $SiMe_4$ occured over a period of hours in benzene-d_6 solution.

Introduction

Complexes that feature multiple bonding between transition metals and carbon, nitrogen, or other main group elements have led to remarkable new stoichiometric and catalytic transformations that have found great utility across numerous disciplines.[1] Although such success prompted tremendous efforts to isolate comparable rare earth analogues, they remained largely elusive until the past two decades. In particular, rare earth complexes bearing a terminal imido functionality (RE = NR, RE = group III and lanthanide elements) were targeted with great enthusiasm, yet prior to 2010 only μ_2- and μ_3-bridging species,[2–4] and complexes wherein a transient RE = NR moiety activates a C–H bond, were reported.[5–7] Accordingly, the discovery by Chen and co-workers that addition of one equivalent of DMAP to the scandium alkylamido complex, $L_1Sc(NHDipp)(CH_3)$ (L_1 = DippNC(CH_3)CHC(CH_3)NCH_2CH_2N(CH_3)$_2$, Dipp = 2,6-$^{i}Pr_2C_6H_3$, DMAP = 4-(CH_3)$_2$NC_5H_4N), affords the terminal scandium imido L_1(DMAP)Sc = NDipp (**1**, Fig. 1) drew considerable attention.[8] Notably, DMAP can be removed by reaction of complex **1** with 9-BBN (9-BBN = 9-borabicyclo(3.3.1)nonane), generating the unstable base-free imide L_1Sc = NDipp, which readily participates in [2 + 2] cycloaddition reactions and activation of C_{sp^2}–H, C_{sp^2}–F, and B–H bonds.[9] The following year Chen demonstrated that methane elimination can be induced in the absence of DMAP if a tethered Lewis base is incorporated into the β-diketiminato ancillary ligand.[10] The

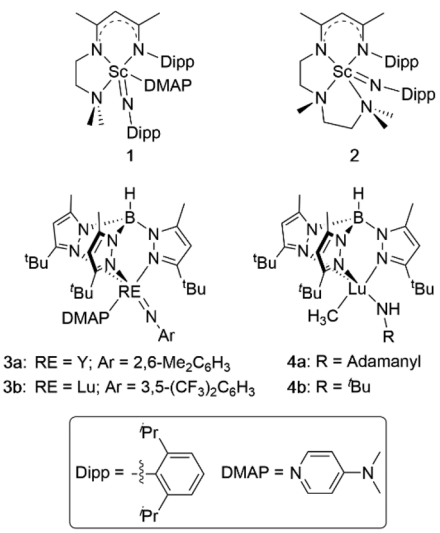

Fig. 1 Selected examples of structurally characterized terminal rare earth imido and alkylamido complexes.

Department of Chemistry and Biochemistry, University of Lethbridge, 4401 University Drive, Lethbridge, AB, Canada, T1K 3M4. E-mail: p.hayes@uleth.ca; Fax: +1403 329 2057; Tel: +1 403 329 2313

†Electronic supplementary information (ESI) available: Including NMR spectra of key compounds and X-Ray Crystallographic Data. CCDC 2417587–2417592, 2423088 and 2429452 for compounds 5–8, 11 and 13. For ESI and crystallographic data in CIF or other electronic format see DOI: **https://doi.org/10.1039/d5dt00338e**

corresponding scandium imide, L_2Sc = NDipp (**2**, L_2 = DippNC$(CH_3)CHC(CH_3)NCH_2CH_2N(CH_3)CH_2CH_2N(CH_3)_2$, Fig. 1), has exhibited rich reaction chemistry with unsaturated organic molecules,[11] main group elements,[10] transition metal coordination complexes,[12] and more.[13] Ultimately, seminal contributions from Chen,[13] Mindiola,[5,6] Piers[7] and Cui[14] demonstrated that given the appropriate system, introduction of either internal or external Lewis bases to a scandium alkylamido complex is an effective strategy for accessing terminal imido functionalities.

Following Chen's approach, Anwander prepared DMAP-stabilized imide complexes of the larger rare earth metals, yttrium and lutetium ($Tp^{tBu,Me}Y$ = N-2,6-$(CH_3)_2C_6H_3$(DMAP) (**3a**, Fig. 1) and $Tp^{tBu,Me}Lu$ = N-3,5-$(CF_3)_2C_6H_3$(DMAP)) (**3b**, Fig. 1) ($Tp^{tBu,Me}$ = HB[3-CH_3-5-^{t}Bu-$N_2C_3H]_3^-$).[15] More recently, Schelter expanded the list of terminal rare earth imides to include the cerium species K[(TriNOx)Ce = N-3,5$(CF_3)_2C_6H_3$] (TriNOx = $N(CH_2$-2-$C_6H_4N(^tBu)O)_3$); Anwander added the dysprosium and holmium complexes $Tp^{tBu,Me}RE$(N-2,6-$^iPr_2C_6H_3$)(DMAP) (RE = Dy, Ho).[16–18] Notably, these examples utilize starting materials that include a mixed methyl/tetramethylgallato system, $Tp^{tBu,Me}RE(Me)(GaMe_4)$ (RE = Y, Dy, Ho), that reacts with H_2NDipp to yield mixed methylamido species primed for imide-formation.

It is important to note that all reported rare earth complexes bearing a terminal imido functionality contain an aromatic group on the imide nitrogen.[4–8,10,14–18] The apparent requirement for aryl substitution piqued our interest, particularly given that neither $Tp^{tBu,Me}Lu(CH_3)$(NHAd) (**4a**, Fig. 1) nor $Tp^{tBu,Me}Lu(CH_3)(NH^tBu)$ (**4b**, Fig. 1), served as appropriate precursors for a lutetium imide.[19] Our group previously synthesized $L^{Ph}Lu(CH_2SiMe_3)(NHCPh_3)$, ($L^{Ph}$ = 2,5-[Ph_2P = N(Pipp)]$_2C_4H_2N^-$, Pipp = 4-$^iPrC_6H_4$) in hopes of observing similar reactivity;[20] however, exhaustive efforts (*e.g.* addition of Lewis or Brønsted bases, heating, *etc.*) failed to yield the targeted imido $L^{Ph}Lu$ = $NCPh_3$. Instead, C_{sp^2}–H activation of the CPh_3 substituent occurred.[20] Herein we utilize the more electron rich NNN-pincer ligand L^{iPr} (L^{iPr} = 2,5-[$^iPr_2P$ = N(Pipp)]$_2C_4H_2N^-$)[21] to alleviate unwanted activations and probe the impact that the amine bound substituent has on rare earth imido synthesis. Furthermore, with the goal of expanding the library of Lewis bases that can promote alkane loss from rare earth alkylamido species, a second NNN-pincer that features 4,6-dimethyl pyrimidine groups, L^{Pm} = [$^iPr_2P$ = N(4,6-$(Me)_2C_4H_4N_2$)]$_2C_4H_2N^-$, was synthesized. Unfortunately, mixed alkylamido lutetium species were unable to be isolated with this ligand, due to spontaneous loss of $SiMe_4$.

Results and discussion

Synthesis of $L^{iPr}Sc(CH_2SiMe_3)_2$ and $L^{iPr}Lu(CH_2SiMe_3)_2$

The dialkyl complexes $L^{iPr}RE(CH_2SiMe_3)_2$ (L^{iPr} = 2,5-[$^iPr_2P$ = N(Pipp)]$_2C_4H_2N^-$), **5** (RE = Sc) and **6** (RE = Lu), were prepared by reaction of HL^{iPr} with $RE(CH_2SiMe_3)_3THF_2$ in toluene for 1 hour (Scheme 1). Production of $L^{iPr}Sc(CH_2SiMe_3)_2$ and $L^{iPr}Lu(CH_2SiMe_3)_2$ was supported by the consumption of ^{1}H and ^{31}P NMR resonances attributed to HL^{iPr}, as well as the emergence of a resonance at δ 0.00 in the ^{1}H NMR spectra that integrated for 12H, attributed to eliminated $SiMe_4$. New single resonances in the $^{31}P\{^1H\}$ NMR spectra (**5** δ 48.0, **6** δ 49.3) similarly support the synthesis of discrete metal complexes in high purity. As previously observed,[21] the P–$(CH(CH_3)_2)_2$ methyl groups are chemically inequivalent on the NMR timescale (**5**: δ 0.93, 0.88, **6**: δ 0.96, 0.85). Like $L^{Ph}Lu(CH_2SiMe_3)_2$, no C_{sp^2}–H bond activation was observed at ambient temperature in solution.[22]

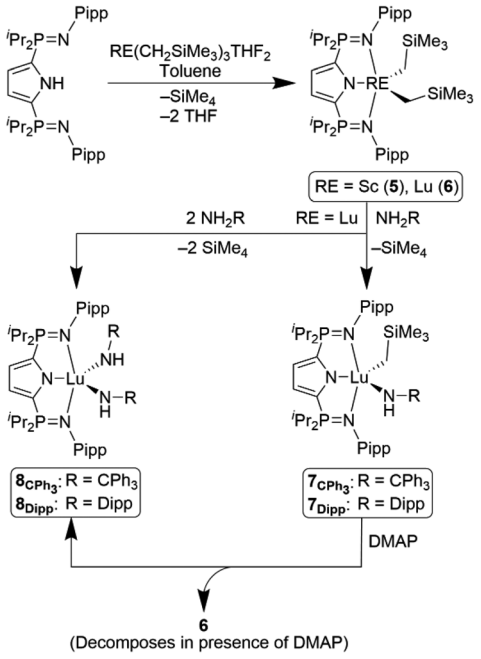

Scheme 1 Synthesis and reactivity of complexes **5** and **6**.

X-Ray diffraction analysis of complexes 5 and 6

Single crystals suitable for diffraction analysis of both complexes **5** and **6** were obtained by slowly cooling warm (50 °C) heptane solutions of each to ambient temperature. Both **5** and **6** crystallized in the $P2_{1/n}$ space group (Fig. 2) and the geometry about each metal centre is best described as distorted square pyramidal (τ^5 = 0.37 (**5**) τ^5 = 0.31 (**6**)). The solid-state structures revealed Lu–C35, Lu–C39, and Lu–N1 distances that were, on average, 0.117 Å longer than those in the scandium congener. As expected, the phosphinimine P–N bond lengths are similar in both complexes (**5**: 1.619(2) Å, **6**: 1.611(3) Å) and elongated relative to HL^{iPr}.[21] These contacts are also comparable to those observed in rare earth complexes supported by the related pincer ligand, L^{Ph} (1.606(4)–1.610(3) Å).[22,23]

Mixed alkylamido lutetium complexes

In order to probe what impact swapping P–Ph_2 for P–$^iPr_2$ groups has on the ability of our ligands to support rare earth terminal imido precursors, complexes **5** and **6** were independently exposed to one equivalent of various primary amines

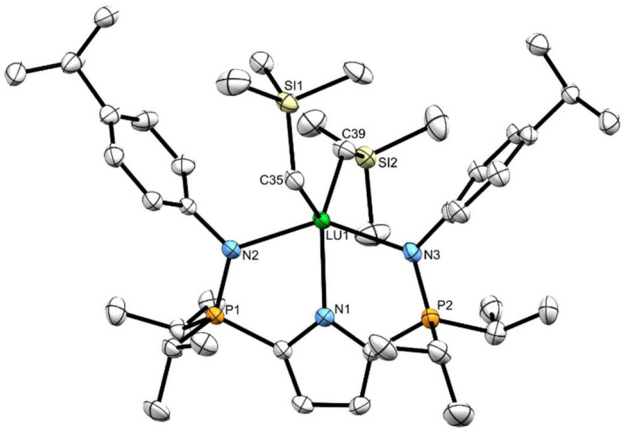

Fig. 2 Solid-state structure of complex **6** with thermal ellipsoids represented at 50% probability. hydrogen atoms omitted for clarity. Selected bond lengths (Å) and angles (°): Lu1–N1 2.305(2), Lu1–N2 2.333 (3), Lu1–C35 2.360(4), P1–N2 1.611(3), C35–Lu1–C39 112.1(1), N2–Lu1–N3 143.79(9), N1–Lu1–C35 125.0(1), N1–Lu1–C39 122.9(1).

(Ph_3CNH_2, $DippNH_2$, $AdNH_2$, or Mes^*NH_2). Unfortunately, compound **5** did not react with Ph_3CNH_2, nor Mes^*NH_2 (Mes^* = 2,4,6-^{t}Bu$_3$C$_6$H$_2$) even upon exposure to heat. Slow, cold addition of 1-adamantylamine ($AdNH_2$) to complex **5** promoted formation of an inextricable mixture of $L^{iPr}Sc(CH_2SiMe_3)_2$ (**5**), $L^{iPr}Sc(CH_2SiMe_3)(NHAd)$, and $L^{iPr}Sc(NHAd)_2$ as indicated by multinuclear NMR spectroscopy. With complex **5** not undergoing successful protonolysis with primary amines, focus was directed to $L^{iPr}Lu(CH_2SiMe_3)_2$ (**6**).

Addition of Ph_3CNH_2 and $DippNH_2$ to compound **6** gave rise to complexes $\mathbf{7_{CPh3}}$, $L^{iPr}Lu(CH_2SiMe_3)(NHCPh_3)$, and $\mathbf{7_{Dipp}}$, $L^{iPr}Lu(CH_2SiMe_3)(NHDipp)$, respectively (Scheme 1). As expected, one equivalent of $SiMe_4$ (δ 0.00) was liberated and observed in both reaction mixtures *via* ^{1}H NMR spectroscopy. Furthermore, a sharp singlet (assigned as the N–*H* resonance), integrating for one proton, which did not give rise to cross peaks in ^{1}H–^{1}H COSY or ^{1}H–^{13}C HSQC experiments, emerged ($\mathbf{7_{CPh3}}$ δ 2.43, $\mathbf{7_{Dipp}}$ δ 4.14). Installation of the $NHCPh_3$/NHDipp ligand produced C_s-symmetric complexes, resulting in the appearance of two sets of P–(C*H*(CH$_3$)$_2$)$_2$ resonances in the ^{1}H NMR spectra of complexes $\mathbf{7_{CPh3}}$ (δ 2.16, 1.75) and $\mathbf{7_{Dipp}}$ (δ 2.26, 1.93). Further evidence for the formation of these mixed alkylamido compounds was provided by the disappearance of the singlet corresponding to $L^{iPr}Lu(CH_2SiMe_3)_2$ (δ 49.3) in tandem with the emergence of a new, resonance ($\mathbf{7_{CPh3}}$ δ 47.9, $\mathbf{7_{Dipp}}$ δ 48.7) in the ^{31}P{^{1}H} spectra. Complexes $\mathbf{7_{CPh3}}$ and $\mathbf{7_{Dipp}}$ were resistant to the intramolecular C–H bond activation reported for our previous generation lutetium alkylamido complex $L^{Ph}Lu(CH_2SiMe_3)(NHCPh_3)$,[20] with no decomposition observed after heating to 70 °C for 72 hours.

X-ray diffraction analysis of $\mathbf{7_{CPh3}}$ and $\mathbf{7_{Dipp}}$

Minimal quantities of warm (50 °C) heptane were used to produce saturated solutions of compounds $\mathbf{7_{CPh3}}$ and $\mathbf{7_{Dipp}}$. The solutions were allowed to cool to ambient temperature before being placed in a −35 °C freezer for 18 hours, yielding X-ray quality crystalline material. The solid-state geometry about the lutetium centres in $\mathbf{7_{CPh3}}$ and $\mathbf{7_{Dipp}}$ is best described as distorted square pyramidal (τ^5 = 0.15 ($\mathbf{7_{CPh3}}$) τ^5 = 0.12 ($\mathbf{7_{Dipp}}$)) with the four nitrogenous atoms forming the square base in each structure (Fig. 3 and 4). Two equivalents of $\mathbf{7_{CPh3}}$ were found within the asymmetric unit; there were no notable structural differences between them.

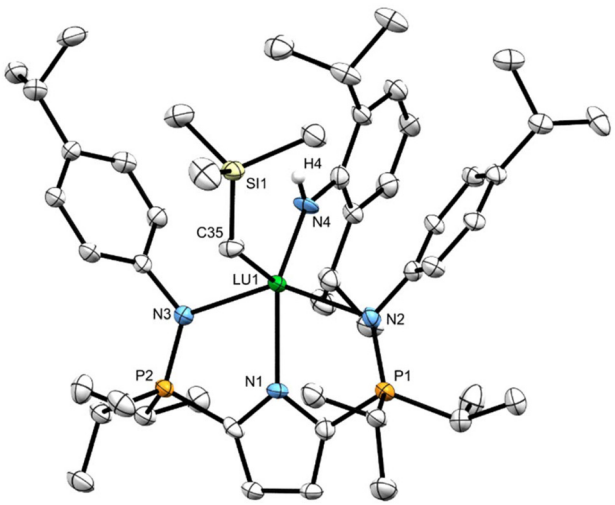

Fig. 3 Solid-state structure for $\mathbf{7_{Dipp}}$ with thermal ellipsoids represented at 50% probability. Hydrogen atoms omitted for clarity. Selected bond lengths (Å) and angles (°) for $\mathbf{7_{Dipp}}$: Lu1–N1 2.283(5), Lu1–N2 2.352(4), Lu1–N3 2.344(5), Lu1–C35 2.313(5), P1–N2 1.625(5), Lu1–N4 2.195(5), C35–Lu1–N4 110.5(2), N3–Lu1–N2 145.3(2). N1–Lu1–N4 138.4(2).

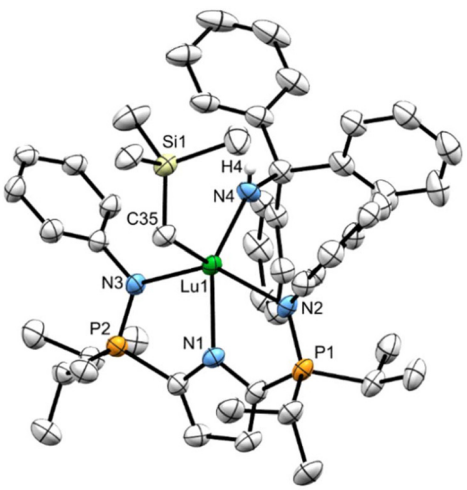

Fig. 4 Solid-state structure for $\mathbf{7_{CPh3}}$ with thermal ellipsoids represented at 50% probability. Hydrogen atoms, Pipp isopropyl groups and one equivalent of $\mathbf{7_{CPh3}}$ have been omitted for clarity. Selected average bond lengths (Å) and angles (°) for $\mathbf{7_{CPh3}}$: Lu1–N1 2.323(2), Lu–N2 2.342 (3), P1–N2 1.617(2), Lu1–C35 2.344(2), Lu1–N4 2.154(2), N3–Lu1–N2 142.9(1), C35–Lu1–N4 105.3(1), N1–Lu1–N4 135.0(1).

The Lu1–C35 bond lengths of complexes 7_{CPh3} (2.342(3) Å) and 7_{Dipp} (2.313(5) Å) are slightly shorter than the Lu–C distances in $L^{iPr}Lu(CH_2SiMe_3)_2$ (Lu1–C35: 2.360(4) Å, Lu1–C39: 2.366(4) Å). However, these distances lie at the low end of Lu–C bonds for published lutetium alkylamido complexes (2.301(4)–2.40(1) Å).[14,15,19,24–29] The phosphinimine P–N bond lengths in both complexes 7_{CPh3} and 7_{Dipp} are not significantly different than those in **6**.

To the best of our knowledge, **4a** ($Tp^{tBu,Me}Lu(CH_3)(NHAd)$), **4b** ($Tp^{tBu,Me}Lu(CH_3)(NH^tBu)$), and $L^{Ph}Lu(NHCPh_3)_2$ represent rare examples of structurally characterized lutetium complexes which possess an amido ligand bearing a non-aromatic substituent.[19,20] Complex 7_{CPh3} exhibits a marginally longer Lu–$NHCPh_3$ bond (2.154(2) Å) than those reported in the literature (2.126(2) Å to 2.144(2) Å for complexes with non-aromatic substituents on nitrogen). Conversely, numerous examples of complexes bearing a monodentate Lu–NHAr (Ar = aromatic) functionality are known, with Lu–NHAr bond lengths ranging from 2.144(3)–2.245(4) Å.[14,15,24–28] The Lu1–N4 distance in complex 7_{Dipp} (2.195(5) Å) falls in the middle of this range. Notably, complex 7_{CPh3} has a shorter Lu1–N4 length of 2.154(2) Å than 7_{Dipp} (2.195(5) Å), despite the large steric presence of the $NHCPh_3$ group (Table 1).

Reactivity with 4-dimethylaminopyridine (DMAP)

Reaction of $L^{iPr}Lu(CH_2SiMe_3)(NHCPh_3)$, 7_{CPh3}, with one equivalent of DMAP promoted slow conversion (12% of compound 7_{CPh3} consumed over 68 hours) to a new product which exhibited a single resonance in the $^{31}P\{^1H\}$ NMR spectrum (δ 45.3). Another 12 hours at ambient temperature did not significantly change the product distribution. Heating this sample to 60 °C for 93 hours produced a dark brown, cloudy solution. This mixture contained a myriad of resonances in the $^{31}P\{^1H\}$ NMR spectrum, with the major product (δ 45.3) comprising 47% of the phosphorous-containing material.

Repeating the experiment at 45 °C resulted in formation of a similar mixture, but this time the resonance at δ 45.3 integrated to only 25% of the material. Increasing the ratio of complex 7_{CPh3} and DMAP to 1 : 2 led to slower consumption of 7_{CPh3} (40% consumed after 4 days), with minimal change to the product mixture.

Exposure of $L^{iPr}Lu(CH_2SiMe_3)(NHDipp)$, 7_{Dipp}, to one equivalent of DMAP at 45 °C for 22.5 hours resulted in 20% consumption of 7_{Dipp} and formation of one major product (δ 46.4) according to the $^{31}P\{^1H\}$ NMR spectrum. Further heating (83.5 hours) resulted in a murky brown solution. In this case, the $^{31}P\{^1H\}$ NMR spectrum revealed that 60% of compound 7_{Dipp} had been consumed and the new resonance appearing at δ 46.4 accounted for 25% of the phosphorous-containing material. In addition, a second substantial resonance (21% by integration) appeared (δ 44.2), in conjunction with a variety of by-products.

Complex 7_{Dipp} was also reacted with two equivalents of DMAP at 45 °C. After 18 hours the $^{31}P\{^1H\}$ NMR spectrum revealed 33% of complex 7_{Dipp} had been consumed, along with concomitant formation of one major product (δ 46.4) accounting for 25% of the phosphorous-containing material. Heating this sample for an additional 145.5 hours resulted in almost complete consumption of 7_{Dipp}, and similar to the equimolar reaction, the resonance at δ 46.4 remained the dominant product (43% of all signals).

Many commonalities were noted when comparing the ^1H NMR spectra for the reactions of 7_{Dipp} and 7_{CPh3} across the various conditions. The unaltered chemical shifts attributed to free DMAP (δ 8.45, 6.07, 2.21) suggested that the Lewis base did not coordinate to the metal centres. Approximately one equivalent of $SiMe_4$ was produced (δ 0.00) and there was no evidence for the retention of any $-CH_2SiMe_3$ functionalities previously attached to the metal centre (complex **6**). The observation of only one P–$(CH(CH_3)_2)_2$ resonance, coupled with the lone signal in the $^{31}P\{^1H\}$ spectra, implies the major product formed in these reactions possesses C_{2v} symmetry. Furthermore, a singlet (δ 4.38 and 2.26) with no cross-peaks in ^1H–^1H COSY experiments grew in each of the reaction mixtures. Diagnostic aromatic resonances pertaining to the $NHCPh_3$ ligand were retained throughout the reaction of

Table 1 Crystallographic table for complexes, 7_{CPh3}, 7_{Dipp}, 8_{CPh3}, and 8_{Dipp} with data for complexes **4b** ($Tp^{tBu,Me}Lu(CH_3)(NH^{tBu})$) and $L^{Ph}Lu(NHCPh_3)_2$ provided for comparison (RE = Sc or Lu)

Parameter	7_{CPh3}	7_{Dipp}	**4b**	8_{CPh3}	8_{Dipp}	$L^{Ph}Lu(NHCPh_3)_2$
Crystal system	Triclinic	Monoclinic	Monoclinic	Triclinic	Monoclinic	Triclinic
Space group	$P\bar{1}$	$P2_1$	$P2_1/n$	$P\bar{1}$	$P2_1/n$	$P\bar{1}$
$R1$ ($I > 2\sigma(I)$)	0.0585	0.0298	0.0211	0.0349	0.0297	0.0311
Selected bond lengths (Å)						
RE1–C35	2.344(2)	2.313(5)	2.362(3)			
RE1–N1	2.323(2)	2.283(5)		2.327(2)	2.280(2)	2.293(4)
P1–N2	1.617(2)	1.625(5)		1.617(3)	1.615(2)	1.620(4)
RE1–N4	2.154(2)	2.195(5)	2.126(2)	2.153(2)	2.176(2)	2.144(2)
Selected bond angles (°)						
N2–RE1–N3	142.9(1)	145.3(2)		143.59(8)	143.76(7)	143.7(1)
N1–RE1–C35	119.65(2)	111.1(2)				
N4–RE1–C35	105.3(1)	110.5(2)	92.81(9)			
N1–RE1–N4	135.0(1)	138.4(2)		132.20(8)	119.68(8)	107.0(1)

complex $\mathbf{7_{CPh3}}$ and DMAP, eventually doubling in integration with respect to DMAP. Similarly, retention and growth of the isopropyl doublet and septet signals pertaining to the NHDipp ligand were observed in the reaction between complex $\mathbf{7_{Dipp}}$ and DMAP. The combination of this evidence led us to believe that the major products of the reaction between complexes **7** and DMAP were the respective bisamide species, $L^{iPr}Lu(NHCPh_3)_2$ ($\mathbf{8_{CPh3}}$) and $L^{iPr}Lu(NHDipp)_2$ ($\mathbf{8_{Dipp}}$). While attempts at isolating these complexes directly from the crude reaction mixtures were unsuccessful, independent synthesis of both $\mathbf{8_{CPh3}}$ and $\mathbf{8_{Dipp}}$ was achieved by addition of two equivalents of NH_2CPh_3 or NH_2Dipp, respectively, to stirring toluene solutions of $L^{iPr}Lu(CH_2SiMe_3)_2$. Heat (70 °C), and additional time (69 hours) was required to prepare $\mathbf{8_{CPh3}}$, compared to $\mathbf{8_{Dipp}}$, which was generated in 24 hours at ambient temperature. Characterization of complexes **8** revealed ^1H and $^{31}P\{^1H\}$ NMR spectra consistent with the major products formed in the reactions of DMAP with complexes $\mathbf{7_{CPh3}}$ and $\mathbf{7_{Dipp}}$. In order to confirm that $\mathbf{8_{CPh3}}$ and $\mathbf{8_{Dipp}}$ were in fact stable products, rather than long lived intermediates prone to decomposition, a sample of $L^{iPr}Lu(NHDipp)_2$ was exposed to 2 equivalents of DMAP at 60 °C for 48 hours, during which no reaction was observed.

In 2004 Piers reported the thermal decomposition of the scandium alkylamido complex $LSc(NH^tBu)(CH_3)$ (L = DippNC(CH_3)CHC(CH_3)NDipp).[30] Upon being heated to 100 °C $LSc(NH^tBu)(CH_3)$ underwent a disproportionation reaction yielding half an equivalent of both $LSc(NH^tBu)_2$ and $LSc(CH_3)_2$, the latter of which decomposed upon formation. A Lewis base induced disproportionation route is proposed as a logical pathway for our systems, with the decomposition of $L^{iPr}Lu(CH_2SiMe_3)_2$ being supported by the elimination of $SiMe_4$. Furthermore, heating (60 °C) a pure sample of $L^{iPr}Lu(CH_2SiMe_3)_2$ (**6**) and DMAP resulted in decomposition and production of myriad products in the $^{31}P\{^1H\}$ NMR spectrum which closely matched the product distribution produced when DMAP was added to $\mathbf{7_{CPh3}}$ or $\mathbf{7_{Dipp}}$ (Scheme 1).

Upon comparison of complexes $\mathbf{7_{CPh3}}$ and $\mathbf{7_{Dipp}}$ with $L_1Sc(NHDipp)(CH_3)$, the alkylamido precursor to Chen's imido **1** (*vide supra*), few substantial structural differences are immediately apparent. The planar arrangement of the three L_1 nitrogen donors matches that observed in complexes **7**, as does the similar N_{amido}–RE–C_{alkyl} bond angle of 103.7(2)° (*cf.* 105.3(1)° and 110.5(2)° in $\mathbf{7_{CPh3}}$ and $\mathbf{7_{Dipp}}$, respectively).[8] Likewise, both $\mathbf{7_{Dipp}}$ and $L_1Sc(NHDipp)(CH_3)$ bear a sterically demanding Dipp group on the amido nitrogen. While the geometries at the metal centres are similar, it should be noted that Chen's complex features the smaller rare earth element, scandium. In addition, the metal in $L_1Sc(NHDipp)(CH_3)$ bears a $-CH_3$, rather than the larger $-CH_2SiMe_3$.

Although Anwander's $Tp^{tBu,Me}$-ligated system supports imidos of different rare earth metals, they too were generated by the elimination of methane. Unfortunately, the substantial differences between the facially capping $Tp^{tBu,Me}$ ligand and our pincer precludes direct structural comparison.[15] With that said, it is worth noting that while Anwander's complexes contain the less sterically demanding 2,6-$(CH_3)_2C_6H_3$ or 3,5-$(CF_3)_2C_6H_3$ groups on the imido nitrogen, aromatic groups were still required.

Perhaps the best comparison to our alkylamido complexes is the phosphazene-based $L_2Sc(CH_2SiMe_3)(NHDipp)$ (L_2 = $N(Ph_2P=NPh)_2$), reported by Cui in 2013 (Scheme 2).[14] In that case, ligand phosphinimine donors, a metal–CH_2SiMe_3 moiety and an NDipp group were common with $\mathbf{7_{Dipp}}$. Though the solid-state structure was not obtained for alkylamido $L_2Sc(CH_2SiMe_3)(NHDipp)$, several striking reactivity patterns were observed. Like complexes $\mathbf{7_{CPh3}}$ and $\mathbf{7_{Dipp}}$, heat led to mixtures of the corresponding bisamido and dialkyl species, the latter of which decomposed with concomitant generation of the proteo ligand HL_2. Nonetheless, addition of DMAP at ambient temperature afforded the terminal scandium imido L_2Sc = NDipp, **9**, though two equivalents of DMAP were deemed necessary. Of particular interest is the fact that when Cui and co-workers attempted the analogous chemistry with lutetium and yttrium alkylamido complexes, no conversion to the corresponding imido species was observed, even when excess DMAP was added.[14] Instead, bisamide species, as well as a mixture of intractable products, formed.

X-ray diffraction analysis of $\mathbf{8_{CPh3}}$ and $\mathbf{8_{Dipp}}$

X-ray quality crystals of independently synthesized $\mathbf{8_{CPh3}}$ and $\mathbf{8_{Dipp}}$ were grown at ambient temperature from saturated warm (50 °C) heptane solutions. Like complexes $\mathbf{7_{CPh3}}$ and $\mathbf{7_{Dipp}}$, the geometry at lutetium in complex $\mathbf{8_{CPh3}}$ (Fig. 5) is best described as distorted square pyramidal (δ^5 = 0.19). The square pyramid in complex $\mathbf{8_{Dipp}}$ (Fig. 6), however, is considerably more distorted (δ^5 = 0.38). This discrepancy in geometry, and the need for heat when preparing $\mathbf{8_{CPh3}}$, is attributed to the large steric influence of the $NHCPh_3$ ligand. Complex $\mathbf{8_{CPh3}}$ possesses a Lu1–N5 bond length of 2.164(3) Å, which is amongst the longest reported for a Lu–NHR species (when $R \neq$ aromatic group).[31] In line with what was observed for complexes $\mathbf{7_{CPh3}}$ and $\mathbf{7_{Dipp}}$, the average Lu–NHDipp bond length in complex $\mathbf{8_{Dipp}}$ (2.191(2) Å) is longer than that in $\mathbf{8_{CPh3}}$ (2.159(2) Å), despite the steric pressure of the CPh_3 substituent (Table 1).

Incorporation of internal Lewis bases

In 2011 Chen demonstrated that an internal Lewis base could stabilize a terminal scandium imido (*vide supra*, $L_2Sc(NDipp)$, **2**).[10] Taking inspiration from those findings, we sought to incorporate internal Lewis bases into our pincer scaffold.

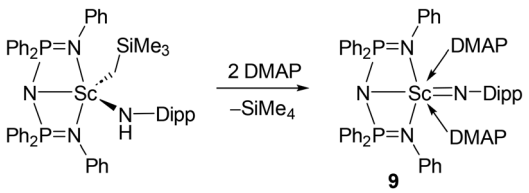

9

Scheme 2 Terminal imido scandium complex **9** reported by Cui and coworkers.

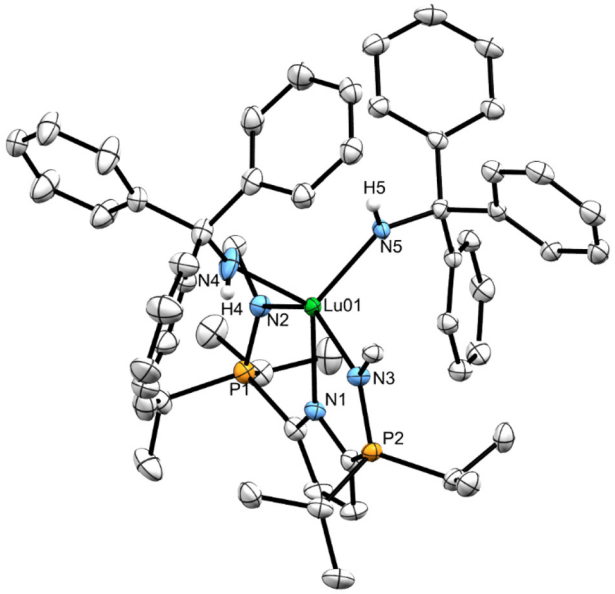

Fig. 5 Solid-state structure for complex $\mathbf{8}_{CPh3}$ with thermal ellipsoids represented at 50% probability.Hydrogen atoms and Pipp groups (except N–C_{ipso} carbon atoms) omitted for clarity. Selected bond lengths (Å) and angles (°) for $\mathbf{8}_{CPh3}$: Lu1–N1 2.327(2), Lu1–N2 2.375(2), Lu1–N4 2.153(2), Lu1–N5 2.164(3), P1–N2 1.617(3), N5–Lu1–N4 103.58(9), N3–Lu1–N2 143.59(8), N1–Lu1–N4 132.20(8), N1–Lu1–N5 124.01(9).

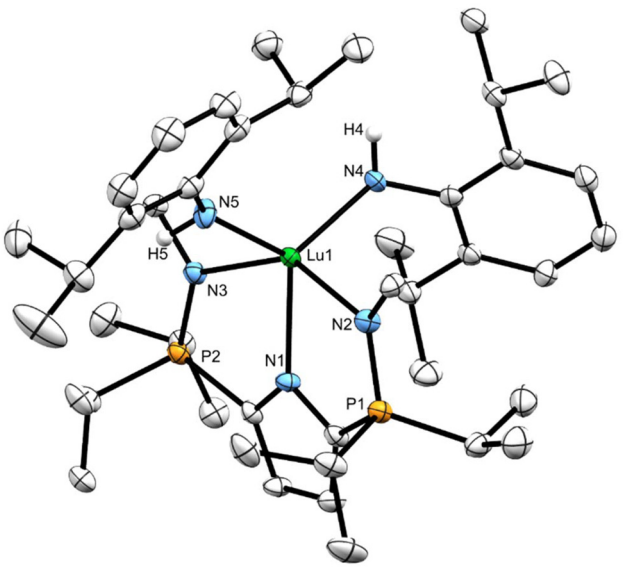

Fig. 6 Solid-state structure for complex $\mathbf{8}_{Dipp}$ with thermal ellipsoids represented at 50% probability. Hydrogen atoms and Pipp groups (except N–C_{ipso} carbon atoms) omitted for clarity. Selected bond lengths (Å) and angles (°) for $\mathbf{8}_{Dipp}$: Lu1–N1 2.280(2), Lu1–N2 2.327(2), Lu1–N4 2.176(2), Lu1–N5 2.206(2), P1–N2 1.615(2), N2–Lu1–N3 143.76 (7), N1–Lu1–N4 119.68(8), N1–Lu1–N5 119.43(7), N4–Lu1–N5 120.78(8).

Addition of three equivalents of NaN_3 to 4,6-dimethyl-2-methylsulfonylpyrimidine in DMF at 100 °C for 3 hours proved an efficient method for producing 2-azido-4,6-dimethylpyrimidine (**10a**, Scheme 3). The valence tautomerization

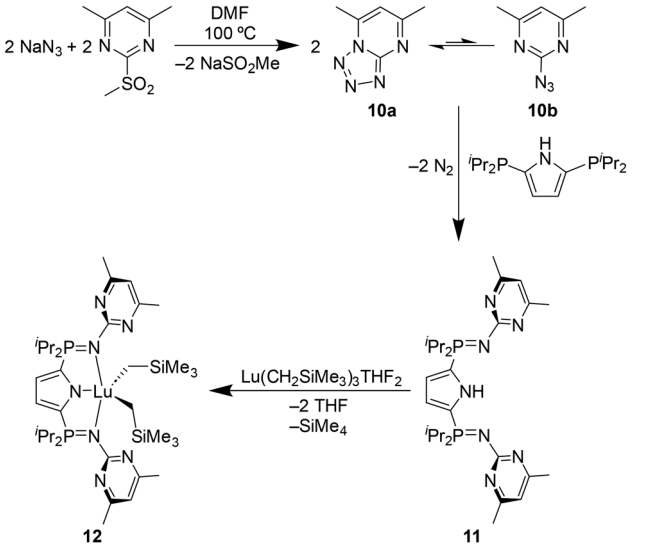

Scheme 3 Synthesis of complex **12**.

observed in the ^{1}H NMR spectrum between compound **10a** and the dominant tetrazole isomer, 5,7-dimethylpyrazolo[1,5a] pyrimidine (**10b**) is consistent with previous reports of this molecule.[32,33]

Formation of HL^{Pm} (**11**) was accomplished by reaction of two equivalents of **10b** with 2,5-bis(diisopropylphosphino)-N–H-pyrrole in toluene (Scheme 3). Likely as a consequence of the equilibrium between **10a** and **10b**, this reaction required additional time compared to the formation of HL^{iPr} (18 hours *vs.* 1 hour). Removal of volatiles *in vacuo* afforded compound **11** as a dark beige powder. The $^{31}P\{^1H\}$ NMR spectrum of the solid revealed one new resonance (δ 29.6). It is worth noting that the methyl substituents of the pyrimidine functionality appear as a singlet in the ^{1}H NMR spectrum (δ 2.35), indicating that free rotation around the $N^{P=N}$–C^{Pm} bond occurs on the NMR timescale. A downfield N–*H* signal (δ 13.2) in the ^{1}H NMR spectrum integrated for one proton and gave rise to no crosspeaks in ^{1}H–^{1}H COSY and ^{1}H–$^{13}C\{^1H\}$ HSQC experiments. This resonance appears substantially further downfield than previously reported N–*H* chemical shifts for our related protio ligands (δ 10.40–12.53),[21,22,34–39] possibly due to hydrogen bonding between N–*H* and the N^{Pm} atoms.

X-ray diffraction analysis of compound 11

A sample of compound **11** was dissolved in a warm (60 °C) 5 : 3 mixture of heptane and toluene, respectively, and allowed to cool to ambient temperature before being placed in a −35 °C freezer for 18 hours, yielding X-ray quality crystalline material. The solid-state structure of compound **11** (Fig. 7), which crystallized in the monoclinic $P2_1/n$ space group, exhibited pyrimidines that lie out of the plane of the pyrrole ring (C1–P1–N2–C23: −57.20°, C4–P2–N3–C17: 173.89°). The phosphinimine (P1–N2 and P2–N3) distances agree well with previously reported compounds.

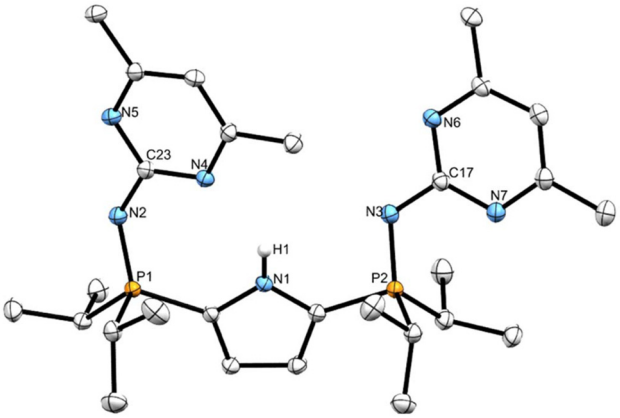

Fig. 7 Solid-state structure for compound **11** with thermal ellipsoids represented at 50% probability. Hydrogen atoms (except H1) omitted for clarity. selected bond lengths (Å) and angles (°) for compound **11**: N1–N4: 2.859(2), P1–N1: 1.588(1), P2–N3: 1.609(1), P1–N2–C23: 129.3(1), P2–N3–C17: 119.7(1), C23–N4–N1: 109.6(1).

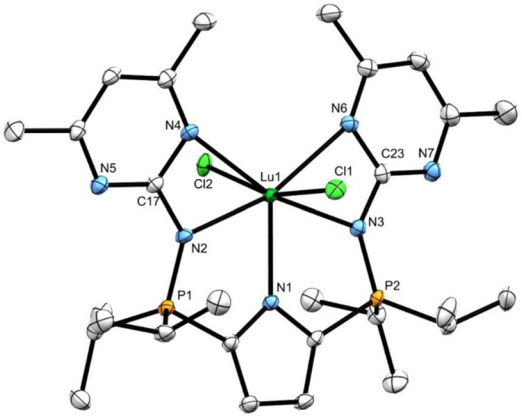

Fig. 8 Solid-state structure for compound **13** with thermal ellipsoids represented at 50% probability. Hydrogen atoms omitted for clarity. Selected bond lengths (Å) and angles (°) for compound **13**: Lu1–N1: 2.324(2), Lu1–N2: 2.318(2), Lu1–N4: 2.546(2), Lu1–Cl2: 2.5808(8). N2–Lu1–N4: 54.59(6), Cl1–Lu1–Cl2: 162.48(3).

Rare earth complexes of ligand 11

To probe the ability of ligand **11** to support well-defined rare earth complexes, a toluene solution containing one equivalent of $Lu(CH_2SiMe_3)_3THF_2$ was added dropwise to a stirring solution of the compound. Analogous to the preparation of $L^{iPr}Sc(CH_2SiMe_3)_2$ and $L^{iPr}Lu(CH_2SiMe_3)_2$ (**5** and **6**, respectively), the resulting solution was allowed to stir for one hour at ambient temperature whereupon all volatiles were removed *in vacuo*, leaving $L^{Pm}Lu(CH_2SiMe_3)_2$ (**12**) as a slightly impure yellow powder (Scheme 3).

Evidence for the formation of complex **12** includes the emergence of a new peak in the $^{31}P\{^1H\}$ NMR spectrum (δ 49.8) along with concomitant disappearance of the phosphorous resonance attributed to **11** (δ 29.6). The pyrimidine-CH_3 groups are no longer chemically equivalent (δ 2.67–1.95) in the ^1H NMR spectrum suggesting slow rotation about the $N^{P=N}$–C^{ipso} bond on the ^1H NMR timescale. A single set of resonances attributed to the lutetium bound alkyl substituents was observed ($CH_2Si(CH_3)_3$: δ 0.11, $CH_2Si(CH_3)_3$: δ −1.04), indicative of a C_s or C_{2v} symmetric product.

Unfortunately, complex **12** spontaneously decomposed in solution at ambient temperature. Production of a small quantity of $SiMe_4$ (δ 0.00) was observed in the ^1H NMR spectrum after 5 minutes. After 24 hours complex **12** had been 35% consumed. Correspondingly, one third of an equivalent of $SiMe_4$ was observed in the ^1H NMR spectrum at that point. Previously we prepared a dialkyl lutetium complex supported by a pincer ligand bearing unsubstituted pyrimidine groups at nitrogen. That species decomposed by alkyl migration from lutetium to pyrimidine, dearomatizing the ring.[39] A similar pathway was reported by Kiplinger in 2006.[40] However, such alkyl migration does not liberate $SiMe_4$, thereby ruling out that mode of decomposition for complex **12**. Unfortunately, repeated attempts to grow X-ray quality crystals of $L^{Pm}Lu(CH_2SiMe_3)_2$, even at low temperature, were unsuccessful. Similarly, the instability of complex **12** precluded both subsequent reaction chemistry and satisfactory combustion analysis.

In an effort to ascertain whether the 4,6-dimethylpyrimidine groups in ligand **11** are likely to stabilize a lutetium imido species by coordinating to the metal, we targeted a dichloride complex expecting a more thermally robust product. To this end, ligand **11** was treated with a stoichiometric quantity of NaH, following protocols established for generating NaL^{iPr}.[21] Subsequent reaction between the sodiated ligand NaL^{Pm} and $LuCl_3(THF)_3$ in THF solution afforded the dichloride complex $L^{Pm}LuCl_2$ (**13**) as a pale yellow solid. Complex **13** displays C_{2v} symmetry in solution at ambient temperature, as indicated by one PC$H$$(CH_3)_2$ methine resonance in the ^1H NMR spectrum and a single ^{31}P peak (δ 52.2). The pyrimidine CH_3 substituents appear as two distinct, signals each integrating to 6H (δ 2.44, 2.05), implying pyrimidine coordination to the metal centre.

X-ray quality crystals of complex **13** were grown from a saturated toluene solution cooled to −35 °C. The solid-state structure determined from X-ray diffraction experiments confirmed that both pyrimidines coordinate to lutetium. Notably, all five nitrogen donors lie approximately in the same plane (P1–N2–C17–N4 torsion angle = 174.3(2)°, P2–N3–C23–N6 torsion angle = 171.46 (2)°; Fig. 8), leading to distorted pentagonal bipyramidal geometry at Lu. The two chlorides, which occupy the apical sites, give rise to a Cl–Lu–Cl angle of 162.48(3)°, which, as expected, is substantially greater than the N_{amido}–Lu–C_{alkyl} angles in the mixed alkylamido complexes **7** (105.3(1), 110.5(2)°) and the N_{amido}–Lu–N_{amido} angles in bisamides **8** (124.01(9), 120.78(8)°).

Conclusions

A series of potential precursors for terminal lutetium imido complexes, $L^{iPr}Lu(CH_2SiMe_3)(NHCPh_3)$ ($\mathbf{7_{CPh3}}$) and $L^{iPr}Lu(CH_2SiMe_3)(NHDipp)$ ($\mathbf{7_{Dipp}}$) were prepared. Unlike our pre-

viously reported lutetium alkylamido complex $L^{Ph}Lu(CH_2SiMe_3)(NHCPh_3)$, which bears phenyl substituents on the ligand's phosphorus atoms,[20] no spontaneous C–H bond activation was observed in solution. Upon addition of DMAP to either $\mathbf{7_{CPh3}}$ or $\mathbf{7_{Dipp}}$ a disproportionation reaction was induced, yielding half an equivalent of $L^{iPr}Lu(CH_2SiMe_3)_2$ and the corresponding bis-amide species $L^{iPr}Lu(NHCPh_3)_2$ or $L^{iPr}Lu(NHDipp)_2$, respectively. The generated $L^{iPr}Lu(CH_2SiMe_3)_2$ rapidly decomposed in the presence of DMAP. Given the paucity of systems similar to ours it is difficult to draw meaningful conclusions regarding what factors dictate imido formation *vs.* ligand redistribution, though greater success has been realized with sterically bulky aromatic substituents on the imido nitrogen and with the smaller metal scandium.

Installation of 4,6-dimethylpyrimidine groups on the iminophosphorane nitrogen atoms of the pincer framework afforded HL^{Pm}, (**11**), a ligand with the potential to stabilize rare earth imido species by coordination of the pyrimidine groups to the metal centre. While addition of $Lu(CH_2SiMe_3)_3THF_2$ to compound **11** generated the expected dialkyl complex $L^{Pm}Lu(CH_2SiMe_3)_2$ (**12**), rapid decomposition at ambient temperature rendered it impossible to prepare desired alkylamido complexes of the form $L^{Pm}Lu(CH_2SiMe_3)(NHR)$. However, preliminary experiments indicate that the rare earth complex $L^{Pm}LuCl_2$ is accessible *via* a salt metathesis route, and notably, *both* pyrimidine groups coordinate to lutetium in the solution and solid states. The possibility of using the amide salts $[[(THF)LiNHCPh_3]_2$ or $[(THF)LiNHDipp]_2)$, to ultimately access alkylamido species that may serve as imido precursors, will be the focus of future studies.

Experimental

General procedures

Manipulation of air- and moisture-sensitive materials and reagents was carried out under an argon atmosphere using vacuum line techniques or in an MBraun glove box. Solvents used for air-sensitive materials were purified using an MBraun solvent purification system (SPS), stored in PTFE-sealed glass vessels over "titanocene" (pentane, benzene, and toluene), and freshly distilled at the time of use. Benzene-d_6 was dried over sodium benzophenone ketyl, de-gassed *via* three freeze–pump–thaw cycles, distilled *in vacuo* and stored over 4 Å molecular sieves in glass bombs under argon. Unless noted, all NMR spectra were recorded at ambient temperature with a Bruker Avance III NMR spectrometer (700.44 MHz for ^{1}H, 176.13 MHz for ^{13}C, and 283.54 MHz for ^{31}P). Chemical shifts are reported in parts per million relative to the external standards $SiMe_4$ (^{1}H, ^{13}C) and 85% H_3PO_4 (^{31}P); residual H-containing species in C_6D_6 (δ 7.16 (^{1}H), δ 128.39 (^{13}C)) were used as internal references. Assignments were aided by the use of $^{13}C\{^1H\}$ DEPT-135, ^1H–$^{13}C\{^1H\}$ HSQC, ^1H–$^{13}C\{^1H\}$ HMBC and ^1H–^1H COSY experiments (s = singlet, d = doublet, t = triplet, q = quartet, sp = septet, m = multiplet, br = broad, ov = overlapping signals). Elemental analyses were performed using an Elementar Vario Micro-cube instrument. The reagents $Lu(CH_2SiMe_3)_3(THF)_2$,[41] $Sc(CH_2SiMe_3)_3(THF)_2$,[42] and 2,5-[^{i}Pr$_2$P = N(4-^{i}PrC$_6$H$_4$)]$_2$NH(C$_4$H$_2$)(HL^{iPr}),[21] were prepared according to literature methods. The compound 2,6-diisopropylanaline was purchased from Sigma Aldrich and distilled under reduced pressure into a bomb equipped with a Kontes valve before using. Compound **10** was synthesized according to literature procedures with additional details provided in the text above.[32,33] All other reagents were purchased from Sigma Aldrich and used without further purification. Unless otherwise specified, reported yields correspond to those obtained for analytically pure samples. When additional purification was required to generate analytically pure compounds for combustion analysis, both the crude and analytical yields are included. In such cases, the reported crude yield corresponds to material that was utilized for successive synthetic steps and was >98% pure as indicated by multinuclear NMR spectroscopy. (N.B. NMR spectra displayed in the ESI† were obtained using these "crude" samples.) It should also be noted that when reported, analytical yields are generally artificially low, as excess crystals grown for X-ray diffraction experiments are used for this purpose. Those recrystallizations were not carried out under conditions that maximize yield, but rather, were optimized for the growth of X-ray quality crystals.

X-Ray crystallography

Crystals grown for X-ray diffraction analysis were coated in Paratone oil and placed on a glass slide. Close visual inspection and selection of the crystals was aided by either a standard microscope or polarizing light microscope. The desired crystal chosen for diffraction analysis was placed on a MiTeGen Dual Thickness MicroMount attached to a goniometer head. The crystal was centred on a Rigaku SuperNova diffractometer equipped with a Dectris Pilatus 3R 200K-A detector, Oxford CryoStream 800 cooling system, molybdenum (NOVA) radiation source (Kα = 0.71073 Å), and copper (MOVA) radiation source (Kα = 1.5406 Å). Experiments were performed at 100 K to reduce thermal motion of the atoms. CrysAlisPro software was utilized to determine unit cell parameters and SHELXTL software was utilized using least squares methodology for refinement.

Synthesis of $L^{iPr}Sc(CH_2SiMe_3)_2$ (5)

A 100 mL round-bottomed flask was charged with a sample of HL^{iPr} (0.0913 g, 0.161 mmol). Toluene (10 mL) was transferred into this flask *via* vacuum distillation, yielding a clear, light brown solution. $Sc(CH_2SiMe_3)_3(THF)_2$ (0.0724 g, 0.161 mmol), was added to a 50 mL round-bottomed flask, and dissolved in toluene (10 mL). The $Sc(CH_2SiMe_3)_3(THF)_2$ solution was added dropwise to the stirring HL^{iPr} solution at ambient temperature over 3 minutes. The resulting clear, light brown solution was left to stir at ambient temperature for 1 hour upon which all volatiles were removed *in vacuo*. The reaction contraption was brought into an inert atmosphere glove box whereupon heptane (10 mL) was added to the light brown solid. The

mixture was stirred and heated (50 °C) leaving behind a small amount of a dark, oily solid. This mixture was filtered through a bed of Celite which produced a clear, yellow solution. Removal of the heptane *in vacuo* liberated the desired product as a light, pale yellow solid (0.113 g, 90.0% (crude)). Facile preparation of analytically pure material was achieved through recrystallization from a minimal amount of warm (50 °C) heptane (0.0521 g, 41.4%). ^{1}H NMR (benzene-d_6): δ 7.50 (dd, $^{3}J_{H-H}$ = 8.4 Hz, $^{4}J_{H-P}$ = 2.1, 4H, *o*-Pipp–H), 7.23 (d, $^{3}J_{H-H}$ = 8.4 Hz, 4H, *m*-Pipp–H), 6.51 (d, $^{3}J_{H-P}$ = 2.1 Hz, 2H, pyrrole–H), 2.80 (sp, $^{3}J_{H-H}$ = 7.0 Hz, 2H, Pipp–(C*H*(CH$_3$)$_2$)), 2.09 (m, $^{3}J_{H-H}$ = 6.9 Hz, $^{2}J_{H-P}$ = 2.7 Hz, 4H, P–(C*H*(CH$_3$)$_2$))), 1.24 (d, $^{3}J_{H-H}$ = 7.0 Hz, 12H, Pipp–(CH(C*H*$_3$)$_2$)), 0.93 (dd, $^{3}J_{H-P}$ = 32.1 Hz, $^{3}J_{H-H}$ = 6.9 Hz, 12H, P–(CH(C*H*$_3$)(CH$_3$))), 0.88 (dd, $^{3}J_{H-P}$ = 31.4 Hz, $^{3}J_{H-H}$ = 6.9 Hz, 12H, P–(CH(CH$_3$)(C*H*$_3$)), 0.31 (s, 4H, Sc–C*H*$_2$SiMe$_3$), 0.16 (s, 18H, CH$_2$Si(C*H*$_3$)$_3$). ^{13}C{^{1}H} NMR (benzene-d_6): δ 145.54 (s, *ipso*-Pipp), 144.57 (s, *ipso*-Pipp), 129.67 (s, *o*-Pipp C–H), 128.41 (d, $^{1}J_{C-P}$ = 24.1, *ipso*-pyrrole) 127.73 (s, *m*-Pipp C–H), 115.90 (dd, $^{2}J_{C-P}$ = 24.1 Hz, $^{3}J_{C-P}$ = 10.1 Hz, pyrrole C–H), 40.00 (br s, Sc–*C*H$_2$), 34.38 (s, Pipp–*C*H(CH$_3$)$_2$), 26.30 (d, $^{1}J_{C-P}$ = 54.0 Hz, P–*C*H(CH$_3$)(CH$_3$)), 24.79 (s, Pipp–CH(*C*H$_3$)$_2$), 16.60 (s, P–(CH(CH$_3$)(*C*H$_3$))), 16.13 (s, P–(CH(*C*H$_3$)(CH$_3$))), 4.65 (s, SiMe$_3$). ^{31}P{^{1}H} NMR (benzene-d_6): δ 48.0. Anal calcd (%) for $C_{42}H_{74}ScN_3P_2Si_2$ C, 64.33; H, 9.51; N, 5.36. Found: C, 64.00, H, 8.79; N, 5.68.

Synthesis of L^{iPr}Lu(CH$_2$SiMe$_3$)$_2$ (6)

A 100 mL round-bottomed flask was charged with a sample of HL^{iPr} (0.1729 g, 0.3040 mmol). Toluene (10 mL) was transferred to this flask *via* vacuum distillation, yielding a clear, light brown solution. Lu(CH$_2$SiMe$_3$)$_3$(THF)$_2$ (0.1766 g, 0.3040 mmol), was added to a 50 mL round-bottomed flask, and was dissolved in toluene (10 mL). The Lu(CH$_2$SiMe$_3$)$_3$(THF)$_2$ solution was added dropwise to the stirring solution at ambient temperature over 3 minutes. The resulting clear, light brown solution was left to stir at ambient temperature for 1 hour upon which all volatiles were removed *in vacuo*. The reaction contraption was brought into an inert atmosphere glove box whereupon heptane (10 mL) was added to the light brown solid. The mixture was stirred and heated (50 °C) leaving behind a small amount of a dark, oily solid. This mixture was filtered through a bed of Celite which produced a clear, yellow solution. Removal of the heptane *in vacuo* liberated the desired product as a pale yellow solid (0.2557 g, 92.01%). Analytically pure material was obtained by recrystallization of the crude sample from a minimal amount of warm (50 °C) heptane (0.1218 g, 43.83%). ^{1}H NMR (benzene-d_6): δ 7.43 (dd, $^{3}J_{H-H}$ = 8.1 Hz, $^{4}J_{H-P}$ = 1.8 Hz, 4H, *o*-Pipp–H), 7.22 (d, $^{3}J_{H-H}$ = 8.1 Hz, 4H, *m*-Pipp–H), 6.50 (d, $^{3}J_{H-P}$ = 2.1 Hz, 2H, pyrrole–H), 2.79 (sp, $^{3}J_{H-H}$ = 6.6 Hz, 2H, Pipp–(C*H*(CH$_3$)$_2$)), 2.04 (m, $^{3}J_{H-H}$ = 7.0 Hz, $^{1}J_{H-P}$ = 2.4 Hz, 4H, P–(C*H*(CH$_3$)$_2$)), 1.22 (d, $^{3}J_{H-H}$ = 6.6 Hz, 12H, Pipp–(CH(C*H*$_3$)$_2$)), 0.96 (dd, $^{3}J_{H-H}$ = 7.0 Hz, $^{2}J_{H-P}$ = 16.2 Hz, 12H, P–(CH(C*H*$_3$)(CH$_3$))), 0.85 (dd, $^{3}J_{H-H}$ = 7.0 Hz, $^{2}J_{H-P}$ = 15.5 Hz, 12H, P–(CH(CH$_3$)(C*H*$_3$))), 0.21 (s, 18H, SiMe$_3$), −0.42 (s, 4H, Lu–C*H*$_2$SiMe$_3$). ^{13}C{^{1}H} NMR (benzene-d_6): δ 144.32 (dd, $^{1}J_{C-H}$ = 98.6 Hz, $^{4}J_{C-H}$ = 24.3 Hz, *ipso*-pyrrole), 129.15 (d, $^{3}J_{C-P}$ = 13.2 Hz, *o*-Pipp C–H), 129.11 (d, $^{2}J_{C-P}$ = 26.4 Hz, *ipso*-Pipp), 127.89 (s, *m*-Pipp C–H), 127.40 (s, *ipso*-Pipp), 116.51 (dd, $^{2}J_{C-P}$ = 98.6 Hz, $^{3}J_{C-P}$ = 40.2 Hz, pyrrole C–H), 41.30 (s, Lu–*C*H$_2$), 34.32 (s, Pipp–(*C*H(CH$_3$)$_2$)), 26.42 (d, $^{1}J_{C-P}$ = 54.0 Hz, P–(*C*H(CH$_3$)$_2$)), 24.76 (s, Pipp–(CH(*C*H$_3$)$_2$)), 16.51 (s, P–(CH(*C*H$_3$)(CH$_3$))), 15.99 (s, P–(CH(CH$_3$)(*C*H$_3$))), 5.19 (s, SiMe$_3$) ^{31}P{^{1}H} NMR (benzene-d_6): δ 49.3. Anal. calcd (%) for $C_{42}H_{74}LuN_3P_2Si_2$ C, 55.18; H, 8.16; N, 4.60. Found: C, 55.01, H, 8.26; N, 4.97.

Synthesis of L^{iPr}Lu(CH$_2$SiMe$_3$)(NHCPh$_3$) (7$_{CPh3}$)

A sample of **6** (0.1033 g, 0.1130 mmol) was weighed into a 20 mL scintillation vial containing a stir bar. The powder was dissolved in 6 mL of toluene, yielding a clear yellow solution. One equivalent of NH$_2$CPh$_3$ (0.0286 g, 0.110 mmol) was added into a 5 mL disposable vial and was dissolved using 2 mL of toluene. The amine solution was added dropwise over 3 minutes to the stirring yellow solution. After stirring at ambient temperature for 1 hour the reaction mixture was filtered through a bed of Celite, eliminating insoluble contaminants. All volatiles were removed *in vacuo* yielding the desired complex as a pale, off-white solid powder (0.103 g, 86.4% yield). X-ray quality crystals were grown at ambient temperature from dissolving the crude powder in a minimal amount of warm heptane (50 °C) (0.0611 g, 51.04% yield). ^{1}H NMR (benzene-d_6): δ 7.53 (m, $^{3}J_{H-H}$ = 3.9 Hz, 6H, *o*-Ph$_3$), 7.08 (ov m, $^{3}J_{H-H}$ = 3.9 Hz, 13H, *m*/*p*-Ph$_3$, Pipp–H), 6.96 (d, $^{3}J_{H-H}$ = 6.3 Hz, 4H, Pipp–H), 6.54 (d, $^{3}J_{H-P}$ = 1.5 Hz, 2H, pyrrole–H), 2.85, (sp, $^{3}J_{H-H}$ = 6.6 Hz, 2H, Pipp–(C*H*(CH$_3$)$_2$)), 2.43 (s, 1H, N–H), 2.16 (dsp, $^{1}J_{H-P}$ = 9.6 Hz, $^{3}J_{H-H}$ = 6.9 Hz, 2H, P–(C*H*(CH$_3$)$_2$)), 1.75 (dsp, $^{1}J_{H-P}$ = 9.6 Hz, $^{3}J_{H-H}$ = 6.9 Hz, 2H, P–(C*H*(CH$_3$)$_2$)), 1.32 (d, $^{3}J_{H-H}$ = 6.6 Hz, 6H, Pipp–(CH(C*H*$_3$)(CH$_3$))), 1.30 (d, $^{3}J_{H-H}$ = 6.6 Hz, 6H, Pipp–(CH(CH$_3$)(C*H*$_3$))), 0.98 (dd, $^{2}J_{P-H}$ = 7.2 Hz, $^{3}J_{H-H}$ = 6.9 Hz, 6H, P–(CH(CH$_3$)(C*H*$_3$))), 0.85 (dd, $^{3}J_{P-H}$ = 7.2 Hz, $^{3}J_{H-H}$ = 6.9 Hz, 6H, P–(CH(C*H*$_3$)(CH$_3$))), 0.77 (d, $^{2}J_{P-H}$ = 6.9 Hz, $^{3}J_{H-H}$ = 6.9 Hz, 6H, P–(CH(CH$_3$)(C*H*$_3$))), 0.61 (dd, $^{3}J_{P-H}$ = 7.2 Hz, $^{3}J_{H-H}$ = 6.9 Hz, 6H, P–(CH(C*H*$_3$)(CH$_3$))), 0.05 (s, 9H, SiMe$_3$), −0.37 (s, 2H, Lu–C*H*$_2$SiMe$_3$). ^{13}C{^{1}H} NMR (benzene-d_6): δ 154.67 (s, *ipso*-CPh$_3$ C), 144.38 (d, $^{1}J_{C-P}$ = 88.5 Hz, *ipso*-pyrrole), 129.60 (s, *ipso*-Pipp) 129.51 (s, Pipp C–H), 128.68 (s, Pipp C–H) 128.24 (*ipso*-Pipp) 127.75 (s, CPh$_3$ C–H), 127.69 (s, CPh$_3$ C–H), 125.91 (s, CPh$_3$ C–H), 116.63 (dd, $^{2}J_{P-C}$ = 24.5 Hz, $^{3}J_{P-C}$ = 9.6 Hz, pyrrole C–H), 75.74 (s, *C*Ph$_3$), 34.39 (s, Lu–C*H*$_2$), 32.60 (s, Pipp–(*C*H(CH$_3$)$_2$)), 26.83 (d, $^{1}J_{P-C}$ = 54.5 Hz, P–(*C*H(CH$_3$)$_2$)), 26.33 (d, $^{1}J_{P-C}$ = 54.5 Hz, P–(*C*H(CH$_3$)$_2$)), 25.02 (s, Pipp–(CH(*C*H$_3$)(CH$_3$))), 24.89 (s, Pipp–(CH(CH$_3$)(*C*H$_3$))), 16.50 (ov s, P–(CH(*C*H$_3$)(CH$_3$))) and P–(CH(CH$_3$)(*C*H$_3$)), 16.49 (s, P–(CH(CH$_3$)(*C*H$_3$))), 16.25 (s, P–(CH(*C*H$_3$)(CH$_3$))), 4.61 (s, SiMe$_3$). ^{31}P{^{1}H} NMR (benzene-d_6): δ 47.8. Anal. calcd (%) for $C_{59}H_{79}LuN_4P_2Si$ C, 63.08; H, 7.34; N, 5.16. Found: C, 62.86, H, 7.12; N, 5.25.

L^{iPr}Lu(CH$_2$SiMe$_3$)(NHDipp) (7$_{Dipp}$)

A sample of **6** (0.1193 g, 0.1305 mmol) was weighed into a 20 mL scintillation vial containing a stir bar. The powder was dissolved in 6 mL of toluene, yielding a clear yellow solution. NH$_2$Dipp (0.0241 g, 0.136 mmol) was weighed into a syringe

and added to a vial containing 5 mL of toluene. This amine solution was then added dropwise to the stirring solution of $L^{iPr}Lu(CH_2SiMe_3)_2$ over 5 minutes. The resulting golden yellow solution was left to stir at ambient temperature for 18 hours whereupon all volatiles were removed *in vacuo*. The resulting pale yellow solid was reconstituted in a minimal amount of a warm (50 °C) 1 : 1 heptane : benzene mixture and recrystallized at −35 °C (0.0722 g, 55.1% yield). ^{1}H NMR (benzene-d_6): δ 7.33 (d, $^3J_{H-H}$ = 7.5 Hz, 2H, *m*-Dipp C–H), 7.22 (dd, $^3J_{H-H}$ = 8.1 Hz, $^4J_{H-P}$ = 1.8 Hz, 4H, *o*-Pipp C–H), 7.01 (d, $^3J_{H-H}$ = 8.1 Hz, 4H, *m*-Pipp C–H), 6.93 (t, $^3J_{H-H}$ = 7.5 Hz, 1H, *p*-Dipp C–H), 6.52 (d, $^3J_{H-P}$ = 2.1 Hz, 2H, pyrrole C–H), 4.14 (s, 1H, N–H), 3.39 (sp, $^3J_{H-H}$ = 6.6 Hz, 2H, Dipp–(C*H*$(CH_3)_2)_2$), 2.73 (sp, $^3J_{H-H}$ = 6.9 Hz, 2H, Pipp–(C*H*$(CH_3)_2$)), 2.26 (m, $^3J_{H-H}$ = 6.9 Hz, $^2J_{H-P}$ = 6.6 Hz, 2H, P–(C*H*$(CH_3)_2$)), 1.93 (m, $^3J_{H-H}$ = 6.9 Hz, $^2J_{H-P}$ = 6.6 Hz, 2H, P–(C*H*$(CH_3)_2$)), 1.35 (d, $^3J_{H-H}$ = 6.6 Hz, 12H, Dipp–(CH$(CH_3)_2)_2$), 1.20 (ov d, $^3J_{H-H}$ = 6.9 Hz, 6H, Pipp–(CH(C*H*$_3$)(CH_3))), 1.19 (ov d, $^3J_{H-H}$ = 6.9 Hz, 6H, Pipp–(CH(CH_3)(C*H*$_3$))), 1.07 (dd, $^3J_{H-H}$ = 6.9 Hz, $^3J_{H-P}$ = 6.9 Hz, 6H, P–(CH(C*H*$_3$)(CH_3))), 0.94 (dd, $^3J_{H-P}$ = 7.2 Hz, $^3J_{H-H}$ = 6.9 Hz, 6H, P–(CH(CH_3)(C*H*$_3$))), 0.80 ((dd, $^3J_{H-H}$ = 6.9 Hz, $^3J_{H-P}$ = 6.9 Hz, 6H, P–(CH(C*H*$_3$)(CH_3)))), 0.74 (dd, $^3J_{H-P}$ = 7.5 Hz, $^3J_{H-H}$ = 6.9 Hz, 6H, P–(CH(CH_3)(C*H*$_3$))), 0.03 (s, 9H, $SiMe_3$), −0.44 (s, 2H, Lu–C*H*$_2$$SiMe_3$). ^{13}C{^{1}H} NMR (benzene-d_6): δ 154.70 (s, *o*-*ipso*-Dipp), 144.56 (s, *ipso*-Pipp), 144.08 (s, *ipso*-Pipp), 133.68 (s, *ipso*-Dipp), 128.33 (dd, $^1J_{C-P}$ = 135.5 Hz, $^3J_{C-P}$ = 14.3 Hz, *ipso*-pyrrole), 128.28 (s, Pipp C–H), 127.82 (s, Pipp C–H), 123.08 (s, *m*-Dipp C–H), 117.20, (dd, $^2J_{C-P}$ = 15.6 Hz, $^3J_{C-P}$ = 10.1 Hz, pyrrole C–H), 114.56 (s, *p*-Dipp C–H), 36.50 (s, Lu–*C*H$_2$), 34.27 (s, Pipp–(*C*H$(CH_3)_2$)), 29.29 (s, Dipp–(*C*H$(CH_3)_2$)), 27.58 (s, P–(*C*H$(CH_3)_2$)), 26.85 (s, P–(*C*H$(CH_3)_2$)), 24.77 (s, Dipp–(CH(*C*H$_3$)$_2$)), 24.70 (s, Pipp–(CH(CH_3)(*C*H$_3$))), 24.58 (s, Pipp–(CH(*C*H$_3$)(CH_3))), 16.84 (s, P–(CH(CH_3)(*C*H$_3$))), 16.59 (ov s, P–(CH(CH_3)(*C*H$_3$))) and P–(CH(*C*H$_3$)(CH_3)), 16.38 (s, P–(CH(*C*H$_3$)(CH_3))), 4.44 (s, $SiMe_3$). ^{31}P{^{1}H} NMR (benzene-d_6): δ 48.7. Anal. calcd (%) for $C_{50}H_{81}LuN_4P_2Si$ C, 59.86; H, 8.14; N, 5.58. Found: C, 59.57, H, 8.11; N, 5.68.

Synthesis of $L^{iPr}Lu(NHCPh_3)_2$ (8_{CPh3})

A 20 mL scintillation vial was charged with $L^{iPr}Lu(CH_2SiMe_3)_2$ (0.0513 g, 0.0561 mmol) and a small stir bar. A second vial was charged with NH_2CPh_3 (0.0291 g, 0.112 mmol). Toluene (7 mL) was added to each flask to dissolve all materials. The NH_2CPh_3 solution was transferred into the $L^{iPr}Lu(CH_2SiMe_3)_2$ solution dropwise *via* Pasteur pipette. The resulting light brown solution was allowed to stir at 70 °C for 69 hours whereupon all volatiles were removed *in vacuo*. The desired product remained as a light brown solid (0.0544 g, 88.7%). X-ray quality crystals were grown by dissolving the mixture in a minimal amount of a warm (50 °C) 1 : 1 mixture of toluene and heptane. The solution was allowed to cool to ambient temperature over 2 hours and was placed in a −35 °C freezer for 16 hours. The resulting crystals were isolated by filtration, washed with cold pentane and dried for 8 hours under vacuum (0.0197 g, 32.1%). ^{1}H NMR (benzene-d_6): δ 7.37 (d, $^3J_{H-H}$ = 7.7 Hz, 12H, *o*-Ph$_3$), 7.08 (ov m, 18H, *m*- and *p*-Ph$_3$), 6.85 (d, $^3J_{H-H}$ = 8.4 Hz, 4H, *o*-Pipp C–H), 6.50 (dd, $^3J_{H-H}$ = 8.4 Hz, $^4J_{H-P}$ = 1.4 Hz, 4H, *m*-Pipp C–H), 6.55 (d, $^3J_{H-P}$ = 2.1 Hz, 2H, pyrrole C–H), 2.83 (sp, $^3J_{H-H}$ = 6.6 Hz, 2H, Pipp–C*H*$(CH_3)_2$), 2.26 (s, 2H, N–H), 1.96 (dsp $^2J_{H-P}$ = 6.6 Hz, $^3J_{H-H}$ = 6.6 Hz, 4H, P–C*H*$(CH_3)_2$) 1.29 (d, $^3J_{H-H}$ = 6.8 Hz, 12H, Pipp–CH(C*H*$_3$)$_2$), 0.81 (dd, $^3J_{H-P}$ = 16.1 Hz, $^3J_{H-H}$ = 6.6 Hz, 12H, P–CH(C*H*$_3$)(CH_3)), 0.79 (dd, $^3J_{H-P}$ = 16.1 Hz, $^3J_{H-H}$ = 6.6 Hz, 12H, P–CH(C*H*$_3$)(CH_3)). ^{13}C{^{1}H} NMR (benzene-d_6): δ 154.38 (s, CPh_3 *ipso*-C), 146.04 (s, *ipso*-Pipp), 142.74 (s, *ipso*-Pipp), 129.98 (s, *o*-CPh_3 C–H), 129.16 (d, $^3J_{C-P}$ = 7.1 Hz, *o*-Pipp C–H), 128.39 (d, $^1J_{C-P}$ = 125.0 Hz, *ipso*-pyrrole), 127.82 (s, *m*-CPh_3 C–H), 127.36 (s, *m*-Pipp C–H), 125.60 (s, *p*-CPh_3 C–H), 116.88 (dd, $^2J_{C-P}$ = 22.9 Hz, $^3J_{C-P}$ = 10.6 Hz, pyrrole C–H), 75.41 (s, *C*Ph$_3$), 34.22 (s, Pipp–*C*H$(CH_3)_2$), 27.03 (d, $^1J_{C-P}$ = 54.6 Hz, P–*C*H$(CH_3)_2$), 24.92 (s, Pipp–CH(*C*H$_3$)$_2$), 16.65 (s, P–CH(*C*H$_3$)(CH_3)), 16.63 (s, P–CH(CH_3)(*C*H$_3$)). ^{31}P{^{1}H} NMR (benzene-d_6): 45.3. Anal. calcd (%) for $C_{72}H_{84}LuN_5P_2$ C, 68.83; H, 6.74; N, 5.57. Found: C, 68.60, H, 7.66; N, 6.31.

Synthesis of $L^{iPr}Lu(NHDipp)_2$ (8_{Dipp})

A round-bottomed flask was charged with $L^{iPr}Lu(CH_2SiMe_3)_2$ (0.1835 g, 0.2007 mmol) and a small stir bar. A second round-bottomed flask was charged with NH_2Dipp (0.0712 g, 0.402 mmol). Toluene (50 mL) was transferred into each flask at −78 °C. The flasks were warmed to ambient temperature whereupon the NH_2Dipp solution was transferred into the $L^{iPr}Lu(CH_2SiMe_3)_2$ solution dropwise *via* syringe. The resulting light brown solution was allowed to stir at ambient temperature for 24 hours whereupon all volatiles were removed *in vacuo*. The desired product remained as a light brown solid (0.184 g, 84.1%). X-ray quality crystals were grown by dissolving the solid in a minimal amount of a warm (50 °C) 1 : 1 mixture of toluene and heptane. The solution was allowed to cool to ambient temperature over 2 hours and was placed in a −35 °C freezer for 16 hours. The resulting crystals were isolated by filtration, washed with cold pentane and dried for 8 hours under vacuum (0.0927 g, 42.3%). ^{1}H NMR (benzene-d_6): δ 7.24 (d, $^3J_{H-H}$ = 7.5 Hz, 4H, *m*-Dipp C–H), 7.06 (dd, $^3J_{H-H}$ = 8.4 Hz, $^4J_{H-P}$ = 2.1 Hz 4H, *o*-Pipp C–H), 6.97–6.88 (ov m, 6H, *m*-Pipp C–H and *p*-Dipp C–H), 6.56 (d, 2H, $^3J_{H-P}$ = 2.4 Hz, pyrrole C–H), 4.38 (s, 2H, N–H), 3.20 (sp, $^3J_{H-H}$ = 6.9 Hz, 4H, Dipp–C*H*$(CH_3)_2$), 2.68 (sp, 2H, $^3J_{H-H}$ = 7.2 Hz, Pipp–C*H*$(CH_3)_2$), 2.09 (dd, $^3J_{H-H}$ = 7.2 Hz, $^2J_{H-P}$ = 1.8 Hz, 4H, P–C*H*$(CH_3)_2$), 1.28 (d, $^3J_{H-H}$ = 6.9 Hz, 24H, Dipp–CH(C*H*$_3$)$_2$), 1.15 (d, $^3J_{H-H}$ = 7.2 Hz, 12H, Pipp–CH(C*H*$_3$)$_2$), 0.91 (dd, $^3J_{H-P}$ = 15.7 Hz, $^3J_{H-H}$ = 7.2 Hz, 12H, P–CH(C*H*$_3$)(CH_3)), 0.79 (dd, $^3J_{H-P}$ = 15.7 Hz, $^3J_{H-H}$ = 7.2 Hz, 12H, P–CH(CH_3)(C*H*$_3$)). ^{13}C{^{1}H} NMR (benzene-d_6): δ 154.42 (s, *ipso*-Dipp), 144.04 (ov s, *ipso*-Pipp and *p*-*ipso*-Pipp), 134.04 (s, *o*-ispo-Dipp), 128.53 (dd, $^1J_{C-P}$ = 134.7 Hz, $^3J_{C-P}$ = 13.7 Hz, *ipso*-pyrrole), 128.45 (d, $^3J_{C-P}$ = 6.4 Hz, *o*-Pipp C–H), 127.65 (s, *m*-Pipp C–H), 122.78 (s, *m*-Dipp C–H), 117.95 (dd, $^2J_{C-P}$ = 17.5 $^3J_{C-P}$ = 9.9 Hz, pyrrole C–H), 114.81 (s, *p*-Dipp C–H), 34.17 (s, Pipp–*C*H$(CH_3)_2$), 29.86 (s, Dipp–*C*H$(CH_3)_2$), 27.40 (d, $^1J_{C-P}$ = 53.6 Hz, P–*C*H$(CH_3)_2$), 24.63 (s, Pipp–CH(*C*H$_3$)$_2$), 24.17 (s, Dipp–CH(*C*H$_3$)$_2$), 16.98 (s, P–CH(CH$_3$)(*C*H$_3$)), 16.54 (s, P–CH(*C*H$_3$)(CH_3)). ^{31}P{^{1}H} NMR (benzene-d_6): δ 46.4. Anal.

calcd (%) for $C_{58}H_{88}LuN_5P_2$ C, 63.78; H, 8.12; N, 6.41. Found: C, 62.82, H, 7.69; N, 7.23.

Synthesis of HL^{Pm} (11)

A sample of 2,5-bis(diisopropylphosphino)-N–H-pyrrole (0.1090 g, 0.3641 mmol) was weighed into a round-bottomed flask and attached to a vacuum line. Two equivalents of 2-azido-4,6-dimethylpyrimidine (**10**) (0.1050 g, 0.7040 mmol) was weighed into a second round-bottomed flask and attached to a vacuum line. Toluene (25 mL) was transferred into each flask at −78 °C. Both solutions were allowed to warm to ambient temperature whereupon a cannula was used to add the solution of compound **10** to the 2,5-bis(diisopropylphosphino)-N–H-pyrrole solution. Bubbles formed shortly after completion of the addition. The solution was left to stir under a constant flow of argon for 18 hours whereupon all volatiles were removed *in vacuo* leaving behind the desired product as a brown solid (0.173 g, 88.3%). X-ray quality crystals were obtained by dissolving the crude product in a minimal amount of toluene in a 20 mL scintillation vial at ambient temperature. Pentane (4 mL) was added to a small, 5 mL vial which was placed inside the vial containing the saturated toluene solution of HL^{Pm}. The entire system was sealed and placed in a −35 °C freezer for 16 hours. The mother-liquor was removed *via* Pasteur pipette and cold (−35 °C) pentane (10 mL) was added to the vial to wash the crystals. The pentane was removed *via* Pasteur pipette and the crystals were dried under vacuum for 2 hours. ^{1}H NMR (benzene-d_6): δ 13.21 (s, 1H, N–H), 6.35 (s, 2H, pyrrole C–H), 6.08 (s, 2H, pyrimidine C–H), 2.39 (spd, 4H, $^3J_{H-H}$ = 7.0 Hz, $^2J_{H-P}$ = 2.6 Hz, P–C*H*$(CH_3)_2$), 2.39 (s, 12H, pyrimidine CH_3), 1.10 (dd, $^3J_{H-P}$ = 16.1 Hz, $^3J_{H-H}$ = 7.0 Hz, P–(CH(C*H*$_3$)(CH$_3$))), 1.00 (dd, $^3J_{H-P}$ = 16.1 Hz, $^3J_{H-H}$ = 7.0 Hz, P–(CH(CH$_3$)(C*H*$_3$))). ^{13}C{^{1}H} NMR (benzene-d_6): δ 168.56 (s, *m-ipso*-pyrimidine), 167.51 (d, $^2J_{C-P}$ = 1.5 Hz, *ipso*-pyrimidine), 124.8 (d, $^1J_{C-P}$ = 41.5 Hz, *ipso*-pyrrole), 116.76 (br s, pyrrole C–H), 109.15 (s, pyrimidine C–H), 26.52 (d, $^1J_{C-P}$ = 65.9 Hz, P–*C*H$(CH_3)_2$), 24.58 (s, pyrimidine CH_3), 17.22 (s, P–(CH(*C*H$_3$)(CH$_3$))), 16.85 (s P–(CH(CH$_3$)(*C*H$_3$))). ^{31}P{^{1}H} NMR (benzene-d_6): δ 27.7. Anal. calcd (%) for $C_{28}H_{44}N_7P_2$ C, 62.09; H, 8.37; N, 18.10. Found: C, 61.36, H, 8.27; N, 17.88.

Synthesis of $L^{Pm}Lu(CH_2SiMe_3)_2$ (12)

A sample of HL^{Pm} (**11**) (0.0580 g, 0.0999 mmol) was weighed into a 20 mL scintillation vial. A disposable shell vial was charged with $Lu(CH_2SiMe_3)_3THF_2$ (0.0552 g, 0.102 mmol). Toluene (3 mL) was added to each vial to dissolve all material. The $Lu(CH_2SiMe_3)_3THF_2$ solution was added to the stirring solution of compound **11** dropwise over 1 minute *via* Pasteur pipette. The clear, pale yellow solution was left to stir at ambient temperature for 1 hour whereupon all volatiles were remove *in vacuo*. Pentane (5 mL) was added to the remaining waxy solid and the mixture was stirred for 15 minutes. The solvent was removed *in vacuo* affording a pale yellow solid (0.0737 g). As complex **12** decomposes slowly in solution, the solid material contained a mixture of predominantly **12** and several intractable impurities. ^{1}H NMR (toluene-d_8): δ 6.62 (d, $^3J_{H-P}$ = 3.5 Hz, 2H, pyrrole C–H), 6.00 (s, 2H, pyrimidine C–H), 2.62–2.56 (ov m, 10H, pyrimidine CH_3 and P–C*H*$(CH_3)_2$), 2.03 (s, 6H, pyrimidine CH_3), 1.22 (dd, $^3J_{H-P}$ = 16.9 Hz, $^3J_{H-H}$ = 7.1 Hz, 12H, P–(CH(C*H*$_3$)(CH$_3$))), 1.02 (dd, $^3J_{H-P}$ = 17.2 Hz, $^3J_{H-H}$ = 7.1 Hz, 12H, P–(CH(CH$_3$)(C*H*$_3$))), 0.02 (s, 18 h, $SiMe_3$), −1.15 (s, 4H, Lu–C*H*$_2$SiMe$_3$). ^{13}C{^{1}H} NMR (toluene-d_8): δ 167.51 (s, *ipso*-pyrimidine), 165.56 (s, *ipso*-pyrimidine), 164.13 (s, *ipso*-pyrimidine), 126.92 (d, $^1J_{C-P}$ = 15.2 Hz, *ipso*-pyrrole), 117.12 (dd, $^2J_{C-P}$ = 26.7 Hz, $^3J_{C-P}$ = 11.2 Hz, pyrrole C–H), 110.98 (s, pyrimidine C–H), 26.37 (s, Lu–*C*H$_2$), 25.85 (d, $^1J_{C-P}$ = 53.8 Hz, P–*C*H$(CH_3)_2$), 23.87 (br s, *endo*/*exo* pyrimidine CH_3), 17.00 (s, P–(CH(*C*H$_3$)(CH$_3$))), 16.08 (s, P–(CH(CH$_3$)(*C*H$_3$))), 5.08 (s, $SiMe_3$). ^{31}P{^{1}H} NMR (benzene-d_6): δ 42.4.

Synthesis of $L^{Pm}LuCl_2$ (13)

A sample of NaL^{Pm} (0.6903 g, 1.225 mmol), synthesized according to the procedure disclosed for preparing NaL^{iPr},[21] was added to a 100 mL two-necked round bottomed flask and attached to a swivel frit apparatus. $LuCl_3(THF)_3$ (0.3486 g, 1.239 mmol) was added to a separate 100 mL round bottom flask. THF (50 mL) was added into each flask *via* vacuum distillation at −78 °C. Each flask was allowed to warm to ambient temperature while stirring. The $LuCl_3(THF)_3$ solution was then added dropwise *via* syringe to the stirring NaL^{Pm} solution over 5 minutes at ambient temperature. The reaction mixture was left to stir at ambient temperature for 3 hours whereupon all volatiles were removed *in vacuo* leaving behind a pale yellow solid. Toluene (50 mL) was transferred into the round bottomed flask *via* vacuum distillation at −78 °C. The solution was allowed to warm to ambient temperature, at which point the NaCl by-product was removed by filtration, affording a clear yellow solution. All volatiles were removed *in vacuo* giving the desired product as a pale yellow solid (0.8207 g, 85.2%). ^{1}H NMR (benzene-d_6): δ 6.68 (d, $^3J_{H-P}$ = 2.4 Hz, 2H, pyrrole C–*H*), 5.90 (s, 2H, aromatic pyrimidine C–*H*), 2.60 (dsp, $^3J_{H-H}$ = 7.2 Hz, $^2J_{H-P}$ = 2.4 Hz, 4H, P–C*H*$(CH_3)_2$), 2.44 (s, 6H, pyrimidine CH_3), 2.04 (s, 6H, pyrimidine C*H*$_3$), 1.29 (dd, $^3J_{H-P}$ = 7.2 Hz, $^3J_{H-P}$ = 17.0 Hz, 12H, P– CH(C*H*$_3$)(CH$_3$)), 1.07 (dd, $^3J_{H-P}$ = 7.2 Hz, $^3J_{H-P}$ = 17.4 Hz, 12H, P–CH(CH$_3$)(C*H*$_3$)). ^{13}C{^{1}H} NMR (benzene-d_6): δ 168.70 (s, pyrimidine *ipso-C*), 166.05 (d, $^2J_{C-P}$ = 5.28 Hz, pyrimidine *ipso-C*), 164.94 (s, pyrimidine *ipso-C*), 128.42 (m, pyrrole *ipso-C*), 117.75 (dd, $^2J_{C-P}$ = 26.0 Hz, $^3J_{C-P}$ = 10.5 Hz, pyrrole *C*–H), 111.64 (s, aromatic pyrimidine *C*–H), 26.16 (d, $^1J_{C-P}$ = 54.4 Hz, P–*C*H$(CH_3)_2$), 24.29 (ov s, pyrimidine *C*H$_3$), 17.09 (s, P–CH(*C*H$_3$)(CH$_3$)), 16.23 (s, P–CH(CH$_3$)(*C*H$_3$)). ^{31}P{^{1}H} NMR (benzene-d_6): δ 52.2. Despite exhaustive efforts, satisfactory combustion data was not obtained.

Author contributions

J. P. K. contributed to investigation, methodology, data curation, formal analysis, writing – original draft and writing – reviewing and editing. S.-J. H. contributed to data curation, formal analysis, writing – reviewing and editing. P. G. H. contributed to conceptualization, funding

acquisition, project administration, formal analysis, supervision, methodology, writing – original draft and writing – reviewing and editing.

Data availability

Original data can be obtained from the authors on request. Deposition Numbers 2417587 (for **5**), 2417588 (for **6**), 2417589 (for $\mathbf{7_{CPh3}}$), 2417590 (for $\mathbf{7_{Dipp}}$), 2417591 (for $\mathbf{8_{CPh3}}$), 2417592 (for $\mathbf{8_{Dipp}}$), 2423088 (for **11**) and 2429452 (for **13**)† contain the supplementary crystallographic data for this paper. These data are provided free of charge by the joint Cambridge Crystallographic Data Centre (CCDC) and Fachinformationszentrum Karlsruche Access Structures service.

Conflicts of interest

The authors have no conflicts to declare.

Acknowledgements

This research was financially supported by a Discovery Grant from the Natural Sciences and Engineering Research Council (NSERC) of Canada. The authors thank Mr Tony Montina and Mr Michael Opyr for expert technical assistance with NMR experiments. Prof. René T. Boeré is gratefully acknowledged for his continued support regarding X-ray diffraction analysis. P. G. H. thanks the University of Lethbridge for a Tier I Board of Governors Research Chair in Organometallic Chemistry.

References

1 O. T. Summerscales and J. C. Gordon, *RSC Adv.*, 2013, **3**, 6682.
2 D. J. Beetstra, A. Meetsma, B. Hessen and J. H. Teuben, *Organometallics*, 2003, **22**, 4372.
3 G. R. Geisbrecht, D. L. Clark, P. J. Hay, D. W. Keogh, R. Poli, B. L. Scott, J. G. Watkin and J. C. Gordon, *Organometallics*, 2002, **21**, 4726.
4 A. A. Trifonov, M. N. Bochkarev, H. Schumann and J. Loebel, *Angew. Chem., Int. Ed. Engl.*, 1991, **30**, 1149.
5 J. Scott, F. Basuli, A. R. Fout, J. C. Huffman and D. J. Mindiola, *Angew. Chem., Int. Ed.*, 2008, **47**, 8502.
6 B. F. Wicker, H. J. Fan, A. K. Hickey, M. G. Crestani, J. Scott, M. Pink and D. J. Mindiola, *J. Am. Chem. Soc.*, 2012, **134**, 20081.
7 T. Chu, W. E. Piers, J. L. Dutton and M. Parvez, *Organometallics*, 2013, **32**, 1159.
8 E. L. Lu, Y. X. Li and Y. F. Chen, *Chem. Commun.*, 2010, **46**, 4469.
9 J. X. Chu, X. H. Han, C. E. Kefalidis, J. L. Zhou, L. Maron, X. B. Leng and Y. F. Chen, *J. Am. Chem. Soc.*, 2014, **136**, 10894.
10 E. L. Lu, J. X. Chu, Y. F. Chen, M. V. Borzov and G. Y. Li, *Chem. Commun.*, 2011, **47**, 743.
11 J. X. Chu, E. L. Lu, Z. X. Liu, Y. F. Chen, X. B. Leng and H. B. Song, *Angew. Chem., Int. Ed.*, 2011, **50**, 7677.
12 J. X. Chu, E. L. Lu, Y. F. Chen and X. B. Leng, *Organometallics*, 2013, **32**, 1137.
13 E. Lu, J. Chu and Y. F. Chen, *Acc. Chem. Res.*, 2018, **51**, 557.
14 W. Rong, J. Cheng, Z. Mou, H. Xie and D. Cui, *Organometallics*, 2013, **32**, 5523.
15 D. Schädle, M. Meermann-Zimmermann, C. Schädle, C. Maichle-Mössmer and R. Anwander, *Eur. J. Inorg. Chem.*, 2015, **2015**, 1334.
16 L. A. Solola, A. V. Zabula, W. L. Dorfner, B. C. Manor, P. J. Carroll and E. J. Schelter, *J. Am. Chem. Soc.*, 2016, **138**, 6928.
17 T. E. Rieser, D. Schädle, C. Maichle-Mössmer and R. Anwander, *Chem. Sci.*, 2024, **15**, 3562–3570.
18 T. E. Rieser, R. Thim-Spöring, D. Schädle, P. Sirsch, R. Litlabø, K. W. Törnroos, C. Maichle-Mössmer and R. Anwander, *J. Am. Chem. Soc.*, 2022, **144**, 4102–4113.
19 D. Schädle, C. Maichle-Mössmer, C. Schädle and R. Anwander, *Chem. – Eur. J.*, 2015, **21**, 662.
20 J. P. Knott, M. M. Hänninen, J. M. Rautiainen, H. M. Tuononen and P. G. Hayes, *J. Organomet. Chem.*, 2017, **845**, 135.
21 C. S. MacNeil, K. E. Glynn and P. G. Hayes, *Organometallics*, 2018, **37**, 3248.
22 K. R. D. Johnson, M. A. Hannon, J. S. Ritch and P. G. Hayes, *Dalton Trans.*, 2012, **41**, 7873.
23 M. T. Zamora, K. R. D. Johnson, M. M. Hanninen and P. G. Hayes, *Dalton Trans.*, 2014, **43**, 10739.
24 K. R. D. Johnson and P. G. Hayes, *Organometallics*, 2011, **30**, 58.
25 T. M. Cameron, J. C. Gordon and B. L. Scott, *Organometallics*, 2004, **23**, 2995.
26 T. M. Cameron, J. C. Gordon, B. L. Scott and W. Tumas, *Chem. Commun.*, 2004, 1398.
27 J. D. Masuda, K. C. Jantunen, B. L. Scott and J. L. Kiplinger, *Organometallics*, 2008, **27**, 1299.
28 R. K. Thomson, M. J. Monreal, J. D. Masuda, B. L. Scott and J. L. Kiplinger, *J. Organomet. Chem.*, 2011, **696**, 3966.
29 S. Zhu, W. Wu, D. Hong, F. Chai, Z. Huang, X. Zhu, S. Zhou and S. Wang, *Inorg. Chem.*, 2024, **63**, 14860.
30 L. K. Knight, W. E. Piers, P. Fleurat-Lessard, M. Parvez and R. McDonald, *Organometallics*, 2004, **23**, 2087.
31 Z.-J. Lv, M. Zhu, W. Liu, Z. Chai, J. Wei and W.-X. Zhang, *Organometallics*, 2021, **40**, 3992.
32 C. Temple and J. A. Montgomery, *J. Org. Chem.*, 1965, **30**, 826.
33 C. Temple, M. C. Thorpe, W. C. Coburn and J. A. Montgomery, *J. Org. Chem.*, 1966, **31**, 935.
34 K. R. D. Johnson and P. G. Hayes, *Organometallics*, 2009, **28**, 6352.

35 K. R. D. Johnson, B. L. Kamenz and P. G. Hayes, *Can. J. Chem.*, 2015, **94**, 330.
36 K. R. D. Johnson and P. G. Hayes, *Inorg. Chim. Acta*, 2014, **422**, 209.
37 K. R. D. Johnson, B. L. Kamenz and P. G. Hayes, *Organometallics*, 2014, **33**, 3005–3011.
38 K. R. D. Johnson and P. G. Hayes, *Dalton Trans.*, 2014, **43**, 2448.
39 K. R. D. Johnson and P. G. Hayes, *Organometallics*, 2013, **32**, 4046.
40 K. C. Jantunen, B. L. Scott, P. J. Hay, J. C. Gordon and J. L. Kiplinger, *J. Am. Chem. Soc.*, 2006, **128**, 6322.
41 A. Arndt, P. Voth, T. P. Spaniol and J. Okuda, *Organometallics*, 2000, **19**, 4690.
42 F. Estler, G. Eickerling, E. Herdtweck and R. Anwander, *Organometallics*, 2003, **22**, 1212.